

## GRAVITY-FED CASTING

C.W. Hirt  
Flow Science, Inc.  
June 1989

### OVERVIEW

---

Gravity-fed castings are those in which metal is poured into a mold. The pouring may be through an opening in the mold wall or into a sprue and then through one or more runners and gates before entering the mold. Generally a riser is provided to hold excess liquid needed to account for solidification shrinkage within the mold.

This type of casting may be characterized as slow in contrast to high pressure filling processes where filling times are typically fractions of a second. In gravity-fed methods more attention must be given to heat transfer processes and possible solidification because of the longer filling times.

In this note we report on a FLOW-3D test calculation for the gravity feeding of a geometrically simple mold. The mold geometry is described in the next section. In the Physical Problem Section it is noted that a special device must be introduced in the geometry in order to model the slow filling rate associated with the gravity feeding system. Computational Results and Summary Comments are contained in the last two sections of the report.

### PHYSICAL PROBLEM

---

The part to be cast consists of a short cylinder (radius=2.0 cm, height=2.0 cm) with four protruding flanges (width=1.0 cm, height=2.0 cm, thickness=0.1 cm) spaced symmetrically around the circumference of the cylinder. Concentric with the first cylinder there is a longer cylinder of smaller radius (radius=1.0 cm, height=3.0 cm). A schematic of the part is shown in Fig. 1. Because of symmetry only one-eighth of the part needs to be modeled (see Fig. 1).

Filling with liquid aluminum takes place through the top of the small diameter cylinder. As originally defined for computational modeling no sprue, riser, or other filling details were given. Instead, a uniform inlet velocity of liquid metal was specified to exist across the entire top of the small diameter cylinder. The velocity of filling was specified as 10 cm/s. If the liquid metal is undergoing free fall, this speed is reached under the action of gravity, and starting from rest, in

a fall of only 0.05 cm. In other words, the inlet velocity is extremely slow, and this causes some difficulties in a numerical model that attempts to have a uniform inflow across the entire top surface of the small cylinder.

The modeling difficulty is really a physical difficulty because in a real system any attempt to establish such a flow across a wide area would quickly become unstable. Spikes of downward moving fluid would form and bubbles of air would move upwards destroying the uniformity of the inlet flow. In the FLOW-3D program one can specify a uniform inlet flow even if it isn't realistic from a physical point of view. However, the consequence of the physical instability is that the fluid is dispersed in small, fast-moving pieces; and the computational results are not very good.

To overcome this inlet problem, one must either use a higher inlet velocity or devise some other strategy that makes better physical sense. It is the latter approach that is used in this report. Wishing to keep the inlet flow rate unchanged we have inserted a horizontal ring baffle a short distance below the inlet (i.e., one computational mesh cell below). Only the central portion of the baffle, of radius 0.38 cm, is open for flow to pass through. This device forces the uniform inlet flow toward the cylinder's axis and, because of the flow area reduction, increases its velocity to about 69.25 cm/s. That this increase in velocity is significant can be appreciated from the fact that fluid freely accelerating through the 3.0 cm length of the small cylinder would acquire a speed of 76.68 cm/s. Thus, with the higher velocity induced by the baffle there is now no possibility for air bubbles to move upward into the fluid above the baffle.

Incoming fluid is assumed to have a temperature of 680° C, while the mold is assumed to remain at a fixed temperature of 50° C. Although the assumption of a fixed-mold temperature is not realistic, it does provide a conservative estimate of solidification effects while filling.

Physical properties of the liquid metal have been taken as:

Density of Solid	2.7 g/cc
Density of Liquid	2.4 g/cc
Specific Heat (Solid & Liquid)	1.0E+7 erg/g/C
Thermal Conductivity (Solid & Liquid)	2.0E+7 erg/s/cm/C
Solidus Temperature	600° C
Liquidus Temperature	640° C
Latent Heat of Fusion	3.95E+9 erg/g
Heat Transfer Coefficient Metal/Mold	1.0E+6 erg/s/cm <sup>2</sup> /C

Because of the magnitude of the inlet velocity and the size of the mold, the effects of viscosity and surface tension are not important and have not been included in the computational model. Such effects can be treated by the FLOW-3D program, but they increase the computational cost; and so these options should not be used when it is known that they cannot have a significant effect on the final results. In this connection it should also be pointed out, for example, that at

the relatively high Reynolds number of this flow (roughly 4000) viscous effects are confined to thin boundary layers and require fine numerical resolution to be correctly modeled. Such fine resolution can significantly increase the computational costs.

## NUMERICAL MODEL

---

Initially it was decided that a cylindrical coordinate system  $(r,\theta,z)$  would be best suited to the geometry. Unfortunately, the heat transfer effects, which include diffusion processes, severely limit the computational time-step size. In particular, it is the small azimuthal cell size near the cylindrical axis that is controlling the time step. Fortunately, however, FLOW-3D can use a Cartesian coordinate system and still represent the geometry. In fact, this system gives better resolution of the thin flanges protruding from the lower cylinder.

The Cartesian mesh (see Fig. 2) consisted of 14 cells in the x direction, 9 cells in the y direction and 15 cells in the z direction. Including boundary cells, the full mesh contained 2992 cells. Although the mesh resolution is limited, it is good for initial calculations of the basic flow structure.

A complete input file for FLOW-3D is given in Fig. 3. This file contains not only the geometric description but all physical and computational parameters necessary to perform the calculation as well as a set of graphic display requests. Of course, the postprocessor in FLOW-3D can be used to obtain other graphic displays after the initial calculation has been completed.

A problem ending time of 1.2 s was estimated as the expected time for filling. As explained in the next section the actual calculation was terminated at 1.05 s when all but a portion of the top cylinder was filled.

## COMPUTATIONAL RESULTS

---

A sequence of perspective plots contained in Fig. 4 shows the filling pattern computed by FLOW-3D. Because of the slow pouring rate, gravity is able to keep the free surface of the metal nearly horizontal. Only relatively small sloshing waves can be seen in these plots. It should be remarked that these plots are contours of the fraction of liquid equal to 0.5, which accounts for the rounding of corners. Also, since the flange region is defined by only one mesh cell (in thickness), it is only the contour in the center of this layer of cells that is plotted, thus giving it the appearance of having no thickness.

The fact that the entire flange region fills with metal is evidence that solidification effects have not taken hold enough to cause serious filling problems. This is further supported by the computed temperature contours described below.

Velocity vectors in the plane containing the flange are shown in Fig. 5. Vectors are drawn out from the center of each cell more than half filled with fluid. A small plus sign, "+", is placed at the base of each vector to indicate fluid-filled cells when the velocity is zero. Here we see even more clearly how gravity keeps the flow under control. During the early stages of filling, say up to  $t=0.8$  s, there is some sloshing evident by the changing flow directions along the bottom of the mold. After 0.8 s, however, the high velocity of the inlet stream (slightly more than 100.0 cm/s) eventually causes a large vortex flow to be generated that extends well into the flange. This, in part, explains why significant solidification does not occur in the flange during filling; i.e., the high temperature incoming fluid is continually being circulated across the flange.

The flow history across the bottom of the mold is given in Fig. 6. There is some recirculation near the entrance to the flange caused by sloshing in the flange, but after 0.8 s the flow is quite uniform.

Figure 7 contains temperature contours at 0.6 s and 1.05 s in both the bottom and flange planes. The lowest temperature in the liquid at the end of the calculation is  $619.4^{\circ}$  C and is located at the outer wall of the flange. Although this value is below the  $640^{\circ}$  C liquidus temperature, it is still well above the  $600^{\circ}$  C solidus temperature.

It may be noted that there is a small amount of cooling of the inlet fluid above the ring baffle where it is in contact with the mold wall, but this is a small effect.

These results indicate that no solidification has occurred during the filling process, at least not on the scale of the mesh resolution used in the calculation. In reality thin layers of solid may have formed along some boundaries, for instance, along the outer vertical wall of the flange. However, any such solidified layers are too thin to be resolved by the computing mesh.

Finally, Fig. 8 shows a contour plot of the wall heat fluxes in the mesh plane containing the flange. Wall heat fluxes only exist in mesh cells containing solids. In this case, since the flange is defined by only one layer of mesh cells, the lower right corner of the plot shows the heat flux through the flange wall in the direction normal to the plot plane. A steep gradient is apparent in these contours at the boundary between the flange and the main cylinder because there is no wall in the center of the cylinder.

The maximum wall heat flux is in the top outer corner of the flange, as would be expected since this corner is exposed to mold walls in three directions.

The calculation was terminated short of complete filling because of the way FLOW-3D defines mesh cells containing free surfaces. For a cell to have a free surface it must have another adjacent cell that is empty of liquid. If a cell is not completely full of liquid and is also not a surface cell, then it is treated as though it is almost filled. In the present problem, because of the limited resolution in the inlet cylinder, the only completely empty cells in the mold are those immediately below the baffle. This situation makes it difficult to obtain pressure convergence. When convergence rates are slow the time-step size is automatically reduced in an effort to improve convergence. Usually this strategy works, but here it didn't and the time step became undesirably small forcing a termination of the problem to avoid wasting computer time.

Several possibilities exist for correcting this computational problem. We could use a different option for the pressure iteration in an attempt to improve the convergence rate, or we could restart the problem with a fixed time-step size so that automatic reductions associated with convergence difficulties would not be introduced. Another possibility, which may be available in the next released version of the code, is to use a simple cavitation model that would treat all non-full cells like surface cells in the sense of their having a fixed pressure (the cavitation pressure). Use of this technique would allow for more complete filling.

## SUMMARY

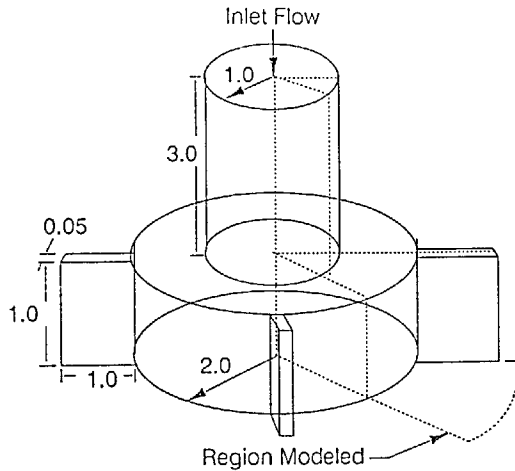
---

This simple problem demonstrates how FLOW-3D can perform an analysis of gravity-fed castings with coupled heat transfer. While geometrically simple, the problem is still difficult because of the complicated free surface configurations developed during the filling process.

It was further shown that some care must be taken in defining the inlet conditions. In particular, inlet conditions should be consistent with physical reality. For the present example this required us to introduce a ring baffle a short distance below the inlet plane.

Even though the filling rate is many times slower than what would be typical in a high pressure filling situation, it is still fast enough that no significant solidification has occurred during the filling.

The computational results consisted of 2435 time cycles to reach a problem time of 1.05 s. On a MicroVAX II computer the total CPU time was 17.54 hours. A SUN 4 workstation or a newer VAX workstation would have performed the calculation approximately four times faster.



All Dimensions in Centimeters

Fig. 1. Schematic of part to be cast.

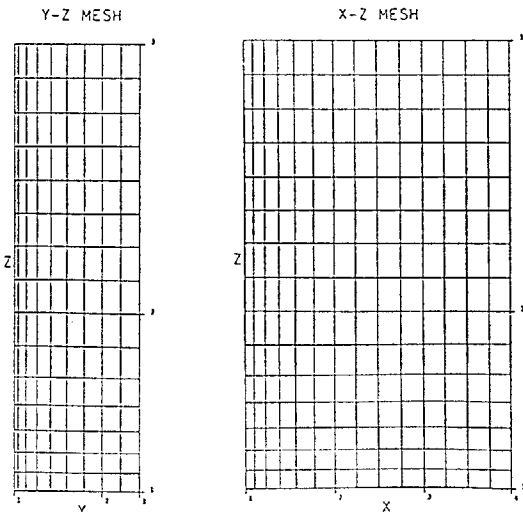
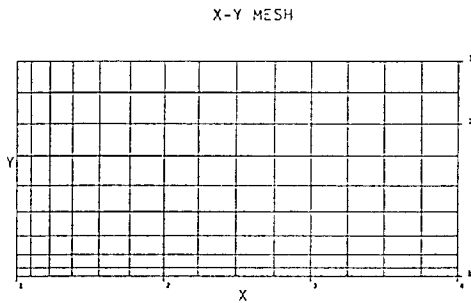


Fig. 2. FLOW-3D Cartesian Mesh.

```

CASTING - RECRUIT
$XPUT
  DELT=0.01, PRTDT=10., PLTDT=0.2, TWFIN=1.2,
  EPSI=.05,
  ITB=1, IFENRG=2, IFRHO=0, IHTC=1, IMPHTC=1,
  IWSH=0, MUI=0.0,
  CZ=-980., AVRCK=-2.1,
  RHOF=2.4,
  CV1=1.0E+7, THC1=2.0E+7, CLHT1=3.95E+9,
  TL1=640., TS1=600., TBCD=50.,
  WL=2, WR=2, WB=2, WT=6,
  WBCT(1,6)=-10.0, FBCT(1,6)=1.0, TBCT(1,6)=680.,
  TBCT(1,2)=50., TBCT(1,5)=50.,
  HWALL1(2)=1.0E+6, HWALL1(5)=1.0E+6,
  IRPR=7, JBKPR=7, KBPR=15,
$END
$MESH
  NXCELT=14,
  PX(2)=1.0, PX(3)=2.0, PX(4)=3.0,
  SIZEX(1)=0.1, NXCELL(1)=6, NXCELL(3)=4,
  NYCELT=9,
  PY(2)=1.0, PY(3)=1.414, SIZEY(1)=0.05,
  NYCELL(1)=7,
  NZCELT=15,
  PZ(2)=2.0, PZ(3)=5.0, SIZEZ(1)=0.2, NZCELL(1)=7,
$END
$OBS
  NOBS=2,
  IOFO(1,1)=1,
  CC(1)=-1.0, RAL(1)=1.0, ZL(1)=2.0,
  IOFO(2,1)=2,
  CC(2)=-1.0, RAL(2)=2.0, ZH(2)=2.0, YL(2)=0.05,
  HOBS1(1)=1.0E+6,
  IOFO(1,2)=3,
  CX(3)=1.0, CY(3)=-1.0,
  ROBS(2)=0.0,
$END
$FL
$END
$BF
  NBAFS=1,
  BCC(1)=-4.621, BCZ(1)=1.0, BRAL(1)=0.38,
$END
$TEMP
$END
$GRAFIC
  NVPLTS=2,
  JV2(1)=2, KV2(2)=2,
  NCPLTS=3,
  JC2(1)=2, KONTYP(1)=5,
  KC2(2)=2, KONTYP(2)=5,
  JC2(3)=2, KONTYP(3)=7,
  NSPLTS=1,
  XEA(1)=10., YEA(1)=20., ZEA(1)=8.0,
$END
$PARTS
$END

```

Fig. 3. FLOW-3D input file.

FREE SURFACE PLOT

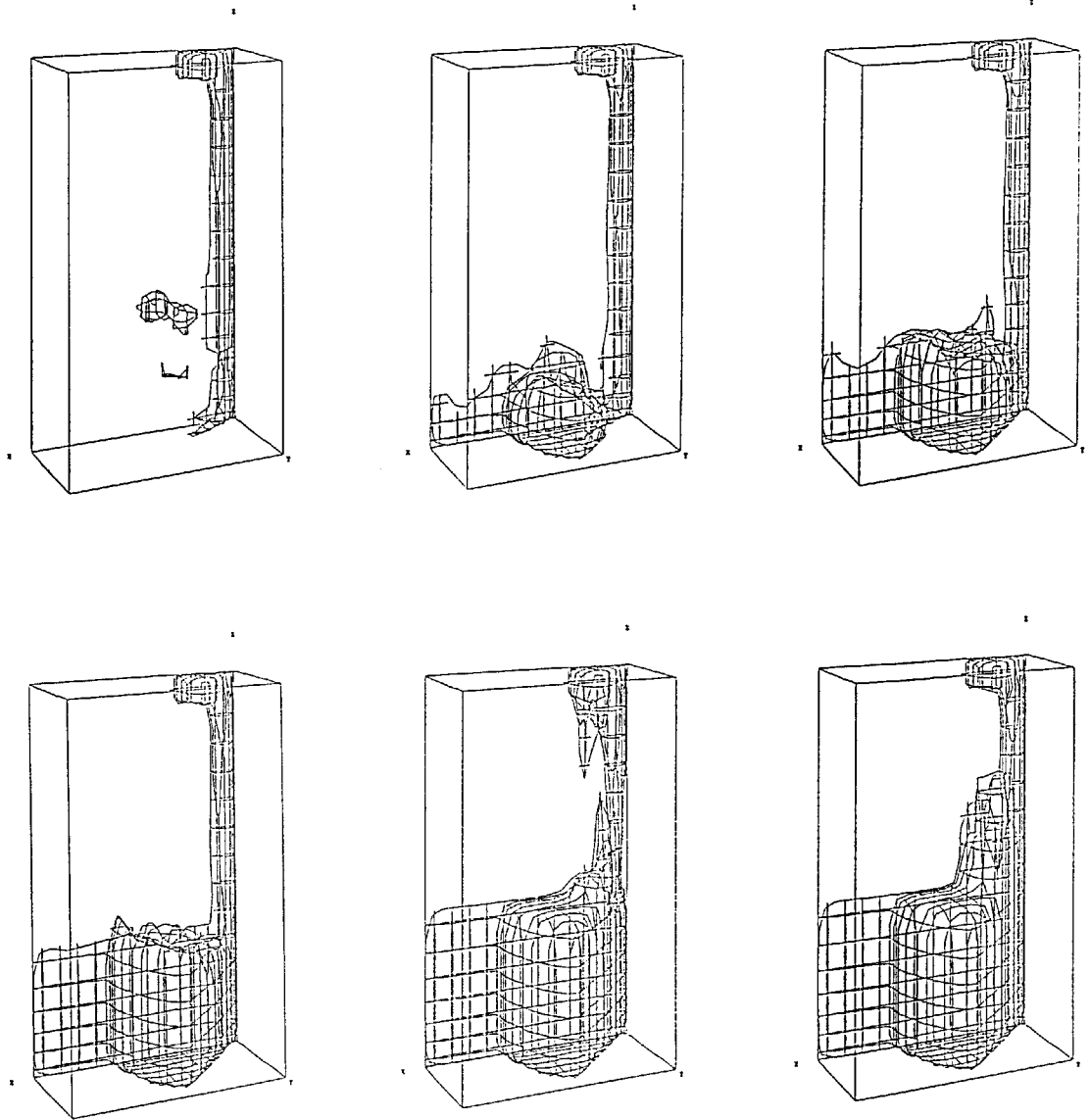


Fig. 4. Perspective plots of liquid filling process.

From left to right and top to bottom times are:  
0.2, 0.4, 0.6, 0.8, 1.0, and 1.05 s.

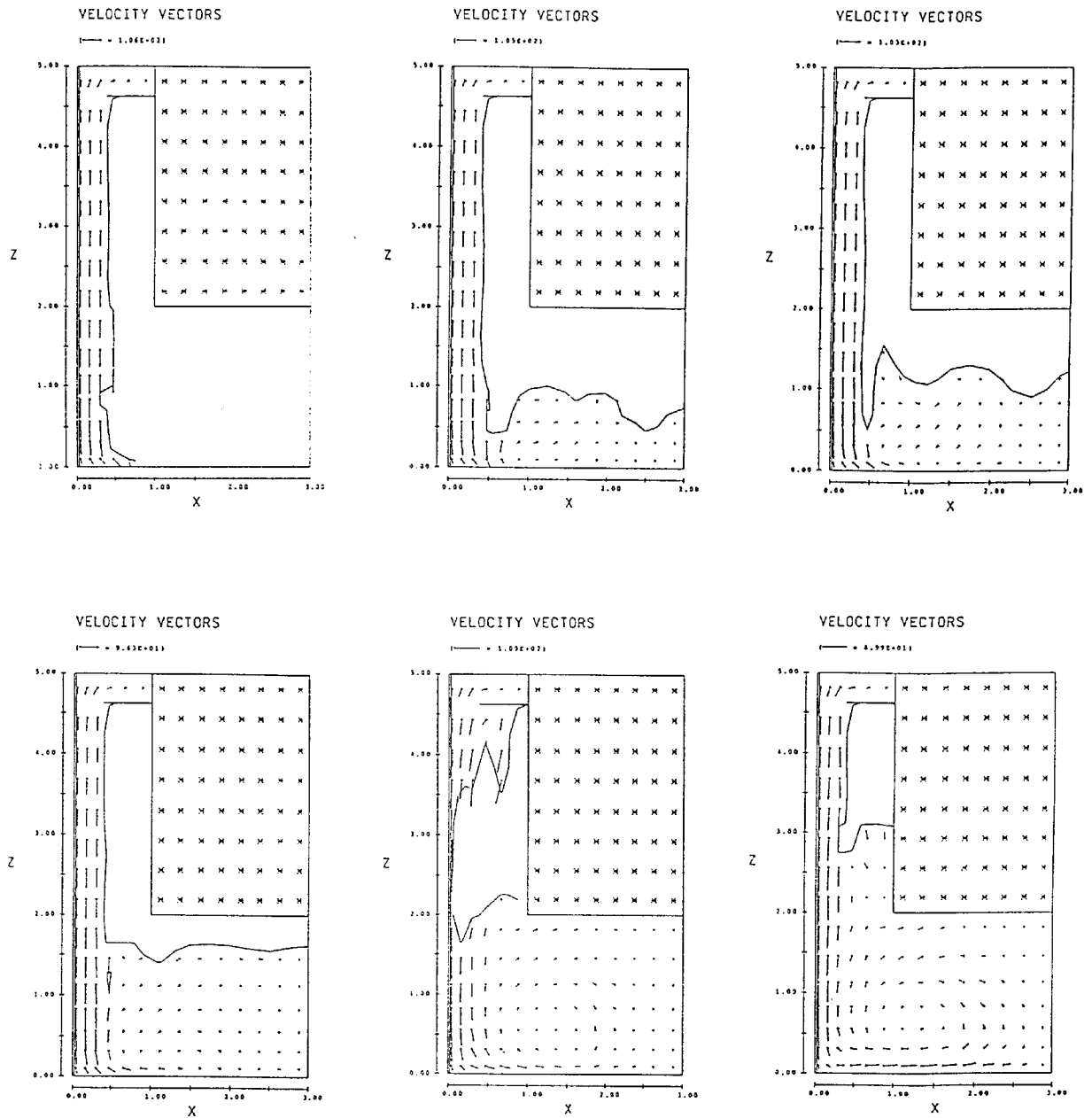


Fig. 5. Vector plots in plane of flange. Same times as in Fig. 4.

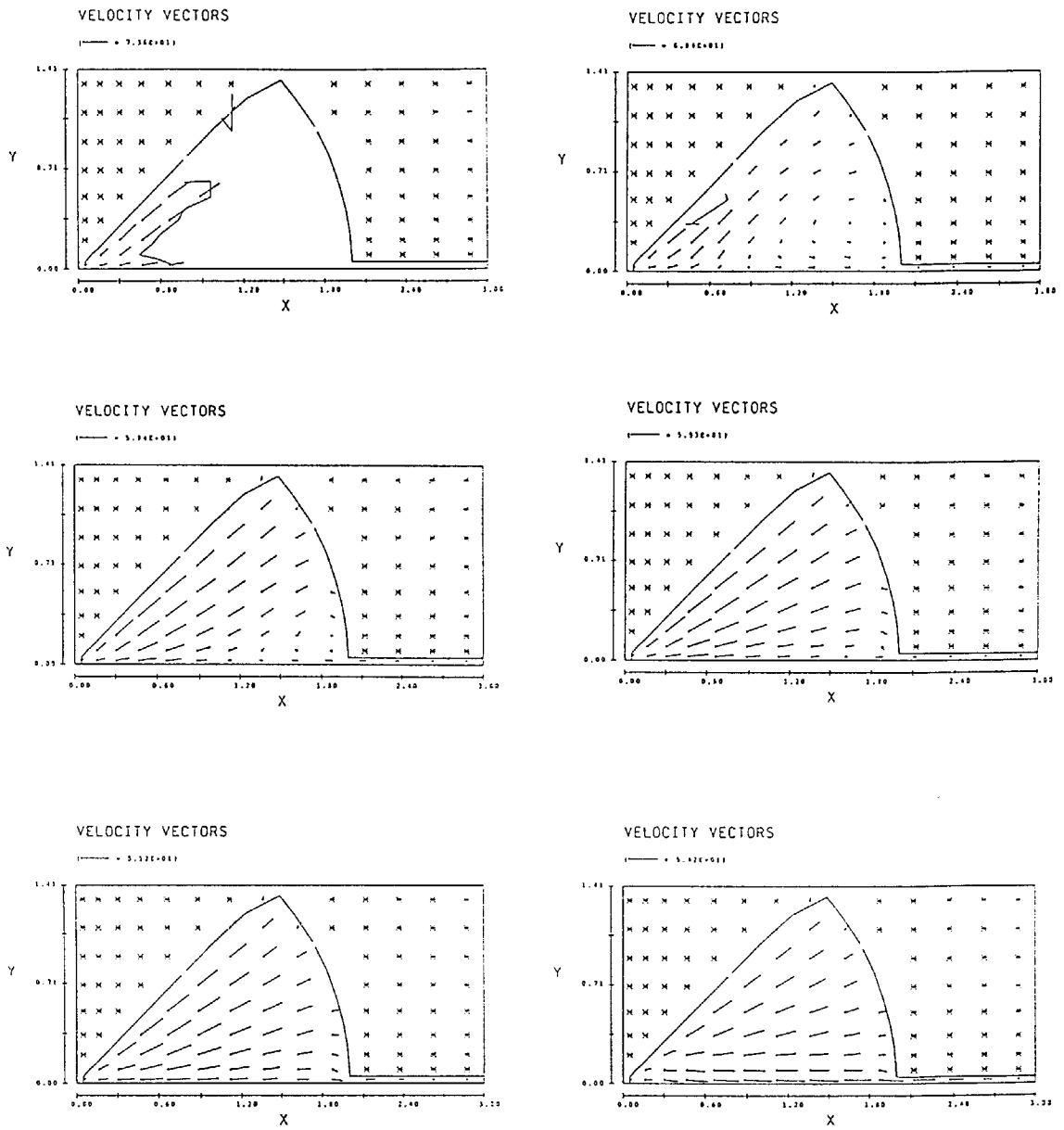
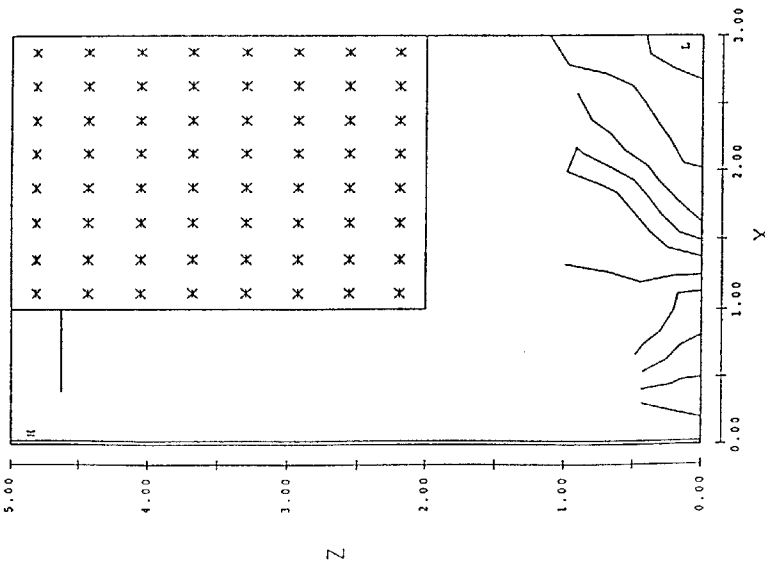


Fig. 6. Vector plots in bottom plane. Same times as in Fig. 4.

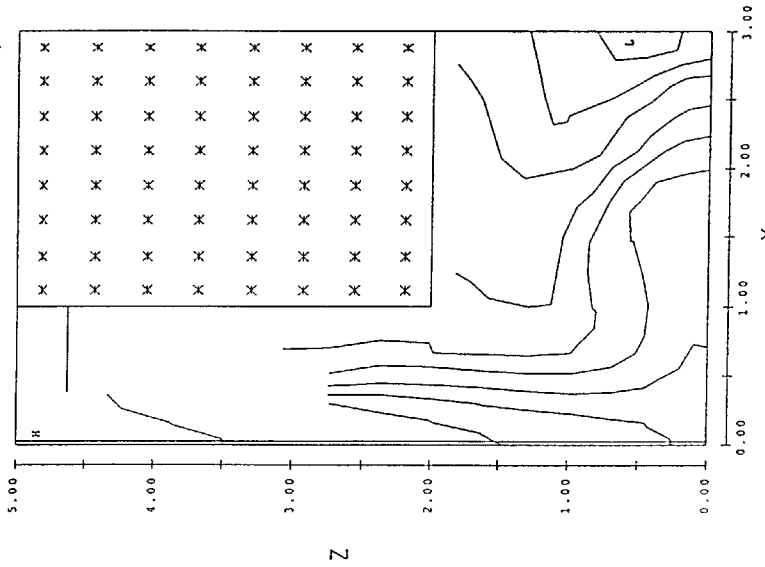
FLUID TEMPERATURE CONTOURS

(LOW= 6.243E+02 LOW CONTOUR= 6.276E+02)  
(HIGH= 6.787E+02 HIGH CONTOUR= 6.760E+02)



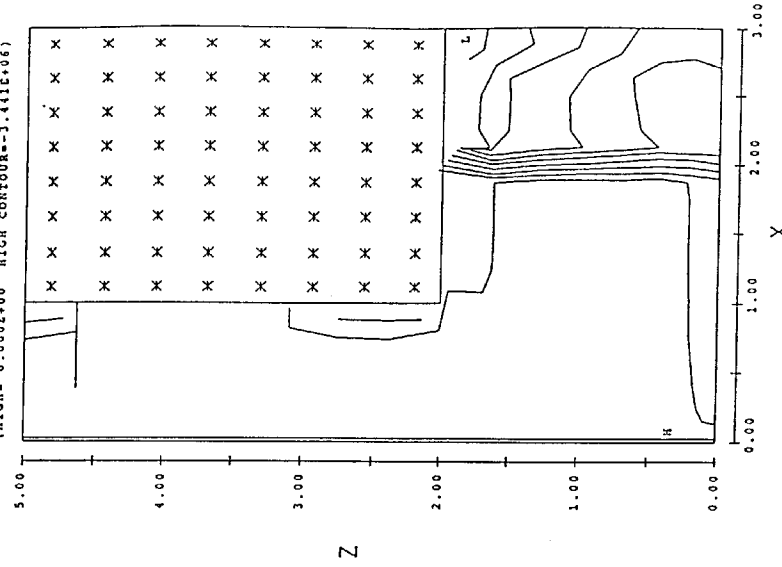
FLUID TEMPERATURE CONTOURS

(LOW= 6.194E+02 LOW CONTOUR= 6.224E+02)  
(HIGH= 6.786E+02 HIGH CONTOUR= 6.756E+02)



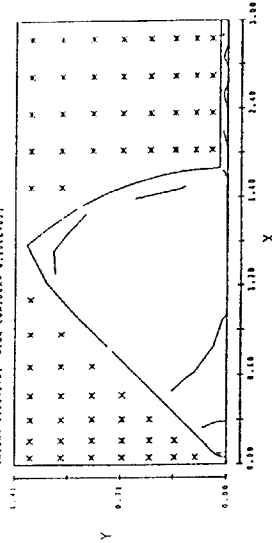
WALL HEAT FLUX CONTOURS

(LOW=-6.882E+07 LOW CONTOUR=-6.538E+07)  
(HIGH= 0.000E+00 HIGH CONTOUR=-3.441E+06)



FLUID TEMPERATURE CONTOURS

(LOW= 6.243E+02 LOW CONTOUR= 6.276E+02)  
(HIGH= 6.787E+02 HIGH CONTOUR= 6.760E+02)



FLUID TEMPERATURE CONTOURS

(LOW= 6.218E+02 LOW CONTOUR= 6.251E+02)  
(HIGH= 6.786E+02 HIGH CONTOUR= 6.756E+02)

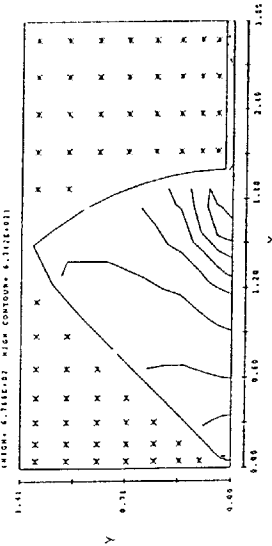


Fig. 8. Wall heat flux contours in layer of mesh cells containing the flange.

Fig. 7. Computed temperature contours in plane of flange (top) and bottom plane (bottom). Times are 0.6 s (left column) and 1.05 s (right column).